



OTC-30975-MS

## Acquire Ocean Bottom Seismic Data and Time-lapse Geochemistry Data Simultaneously to Identify Compartmentalization and Map Hydrocarbon Movement

Rick Schrynemeeckers, Amplified Geochemical Imaging, LLC

Copyright 2021, Offshore Technology Conference

This paper was prepared for presentation at the Offshore Technology Conference held in Houston, Texas, USA, 16-19 August 2021.

This paper was selected for presentation by an OTC program committee following review of information contained in an abstract submitted by the author(s). Contents of the paper have not been reviewed by the Offshore Technology Conference and are subject to correction by the author(s). The material does not necessarily reflect any position of the Offshore Technology Conference, its officers, or members. Electronic reproduction, distribution, or storage of any part of this paper without the written consent of the Offshore Technology Conference is prohibited. Permission to reproduce in print is restricted to an abstract of not more than 300 words; illustrations may not be copied. The abstract must contain conspicuous acknowledgment of OTC copyright.

---

### Abstract

Current offshore hydrocarbon detection methods employ vessels to collect cores along transects over structures defined by seismic imaging which are then analyzed by standard geochemical methods. Due to the cost of core collection, the sample density over these structures is often insufficient to map hydrocarbon accumulation boundaries.

Traditional offshore geochemical methods cannot define reservoir sweet spots (i.e. areas of enhanced porosity, pressure, or net pay thickness) or measure light oil or gas condensate in the C<sub>7</sub> – C<sub>15</sub> carbon range. Thus, conventional geochemical methods are limited in their ability to help optimize offshore field development production.

The capability to attach ultrasensitive geochemical modules to Ocean Bottom Seismic (OBS) nodes provides a new capability to the industry which allows these modules to be deployed in very dense grid patterns that provide extensive coverage both on structure and off structure. Thus, both high resolution seismic data and high-resolution hydrocarbon data can be captured simultaneously.

Field trials were performed in offshore Ghana. The trial was not intended to duplicate normal field operations, but rather provide a pilot study to assess the viability of passive hydrocarbon modules to function properly in real world conditions in deep waters at elevated pressures. Water depth for the pilot survey ranged from 1500 – 1700 meters.

Positive thermogenic signatures were detected in the Gabon samples. A baseline (i.e. non-thermogenic) signature was also detected. The results indicated the positive signatures were thermogenic and could easily be differentiated from baseline or non-thermogenic signatures.

The ability to deploy geochemical modules with OBS nodes for reoccurring surveys in repetitive locations provides the ability to map the movement of hydrocarbons over time as well as discern depletion affects (i.e. time lapse geochemistry). The combined technologies will also be able to:

- Identify compartmentalization,
- maximize production and profitability by mapping reservoir sweet spots (i.e. areas of higher porosity, pressure, & hydrocarbon richness),

- rank prospects,
- reduce risk by identifying poor prospectivity areas,
- accurately map hydrocarbon charge in pre-salt sequences,
- augment seismic data in highly thrust and faulted areas.

## Introduction

Historically, geochemical evaluations of offshore petroleum systems have occurred through the analysis of core samples collected over structures defined from seismic imaging, see Figure 1. Due to the cost of core collection, the sample density over these structures is usually insufficient to map hydrocarbon accumulation boundaries. As such, these surveys answer three questions: 1. Are active petroleum systems present? 2. What is the phase or thermal maturity of the detected hydrocarbons? and 3. How do detected thermogenic hydrocarbons relate to regional petroleum systems? Given the small number of samples involved (typically 100 – 200), and limited coverage over the structure, the geochemical data cannot answer additional important questions such as:

- Is there compartmentalization?
- What are the boundaries of accumulations?
- Where are the field Sweet Spots (i.e. the best porosity, pressure & hydrocarbon richness)?
- Can you rank the prospectivity of the various structures?

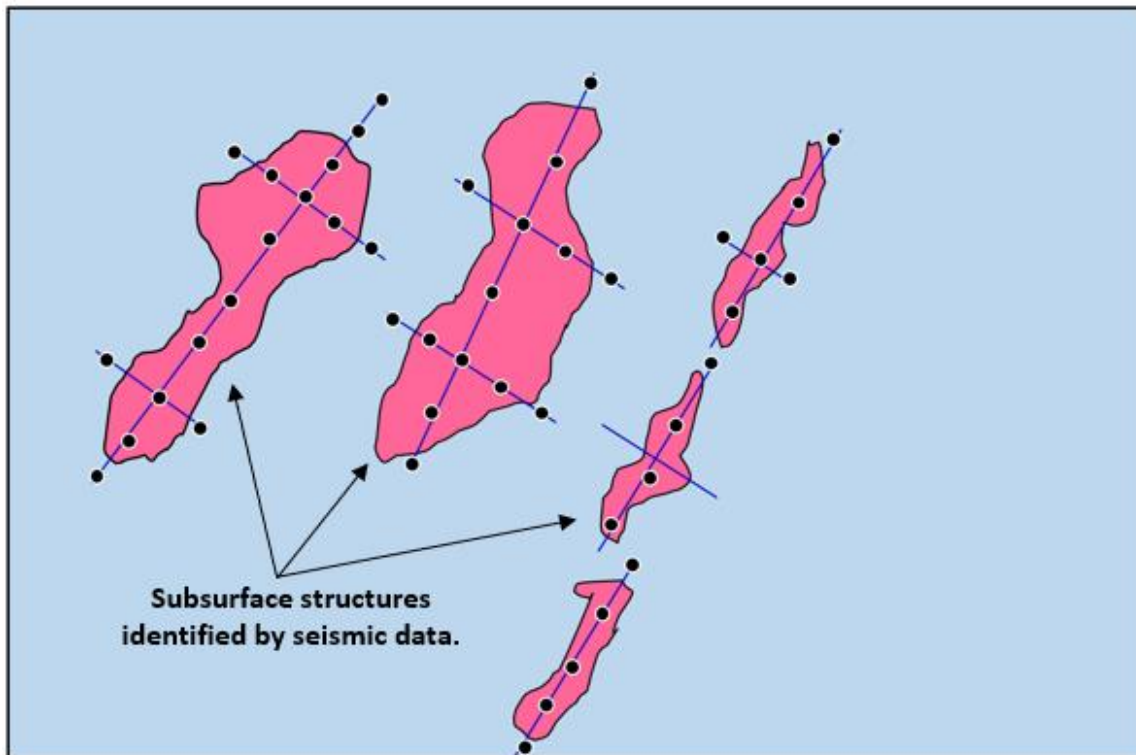


Figure 1. This image illustrates typical geochemical coring campaigns. The pink polygons represent subsurface structures as identified from seismic imaging. The black dots represent coring locations along transects.

High resolution geochemical grid surveys have been employed onshore for well over 25 years to answer these questions but have not been feasible offshore due to the fact there has not been a viable deployment

mechanism for the passive geochemical sorbers. As such, ultrasensitive geochemical methods have been restricted to the analysis of cores from coring campaigns.

However, attaching ultrasensitive geochemical passive modules to Ocean Bottom Seismic (OBS) nodes now provides a new option to the industry. Attaching them to OBS nodes allows the modules to be deployed in a dense grid pattern that provides extensive coverage over structures to map hydrocarbon charge, see Figure 2. This capability allows for the simultaneous acquisition of high-resolution seismic data and high-resolution geochemical data.

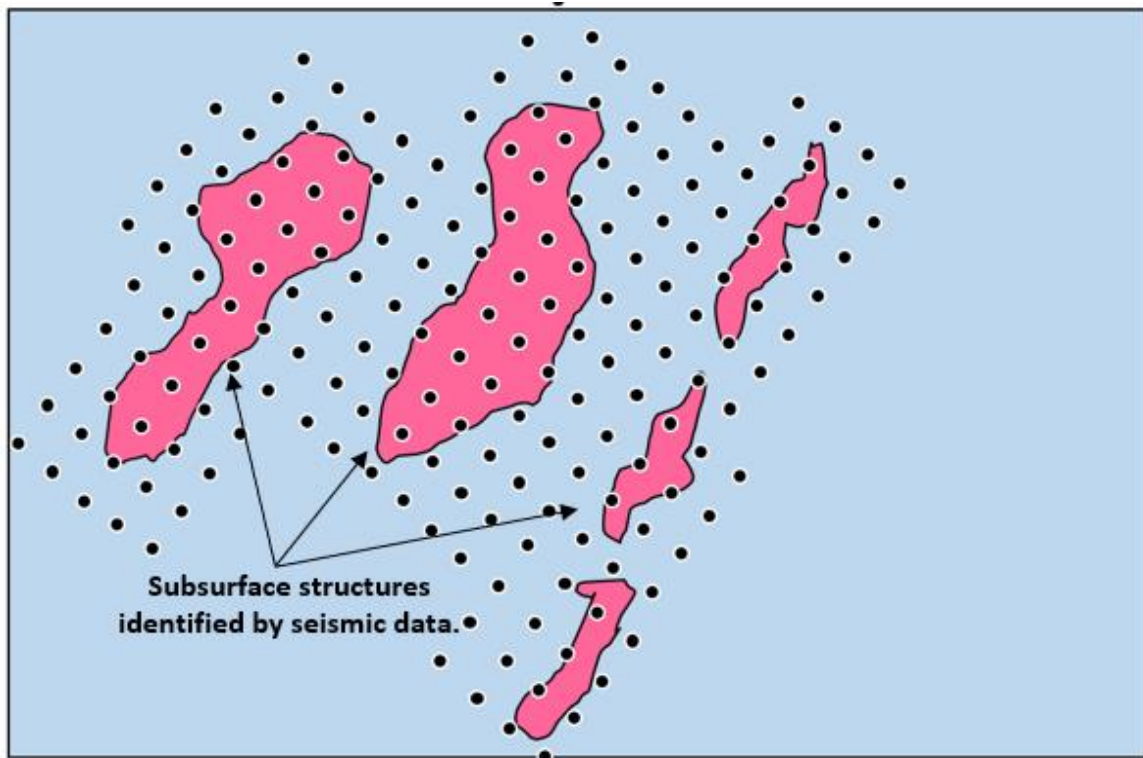


Figure 2. This image illustrates deployment of ultrasensitive passive geochemical modules attached to OBS nodes. The pink polygons represent subsurface structures as identified from seismic imaging. The black dots represent module locations. Note the extensive coverage of geochemical sensors both on structure and off structure.

## Methods, Procedures, & Processes

In microseepage hydrocarbon compounds pervade the overlying seal and migrate vertically through the stratigraphic sequence to the surface (Price, 1986; Klusman, 1993; Klusman and Saeed, 1996; Jones and Burtell, 1996), see Figure 3. The leakage is not massive, as compared to a breach of a structural closure. This process is distinct from the movement of hydrocarbons along breaching faults or fracture swarms (i.e. macroseepage), with its consequent surface expression of an oil or gas seep (Rostron and Toth, 1996; Saunders, 1999; Silliman, 2005).

It is important to note that the migration of microseepage hydrocarbon compounds, unlike macroseepage, is nearly vertical in direction (Davidson, 1982; Davidson, 1985; Rice, 1996); thus, the surface expressions of these compounds overlay the subsurface accumulations. Microseepage rates typically range from 1 m – 3 m per day, reflecting real-time reservoir conditions below (Araktingi, 1984).

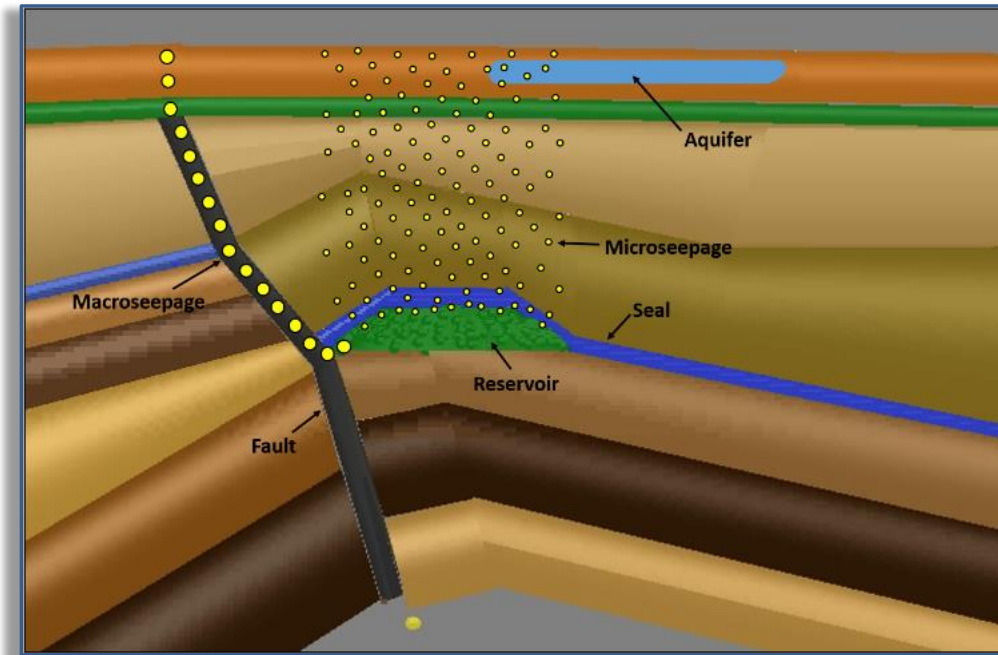


Figure 3. In this diagram the green section represents the reservoir and the horizontal blue line on top of the reservoir represents the seal. The thick gray vertical line next to the reservoir represents a fault. Hydrocarbons from macroseepage travel along faults and find their way to the surface and are present at percent levels. Macroseep surface expressions are normally off set from their source. Microseepage occurs when individual hydrocarbon molecules in the reservoir migrate through the seal along grain boundaries and microfractures. These gas molecules are lifted, essentially vertically, to the seabed floor by microbuoyancy.

There are three primary factors that drive microseepage: reservoir pressure, reservoir porosity, and net pay thickness. The greater the combination of these three factors, the stronger the hydrocarbon signal at the seabed floor. However, the concentration of microseepage hydrocarbons occur at parts per billion (*ppb*) concentrations (Silliman, 2005; Schrynmeeckers, 2011). Consequently, unique techniques are required to accurately and reproducibly measure hydrocarbon compounds at these minute levels.

Detection of these *ppb* hydrocarbon concentrations is accomplished using a proprietary passive sampler, see Figure 4, which contains a specially engineered oleophilic (i.e. oil loving) adsorbent encased in a microporous membrane. Membrane pores are small enough to prevent soil particles from entering, but large enough to allow hydrocarbon molecules to pass through and concentrate on the adsorbent within, resulting in detection levels which are approximately 1,000-fold lower than traditional methods. Since the analytical method measures ~ 88 compounds from  $C_2 - C_{20}$ , it has the unique ability to clearly define and differentiate multiple gas, gas condensate, or oil hydrocarbon signatures, see Figure 5.

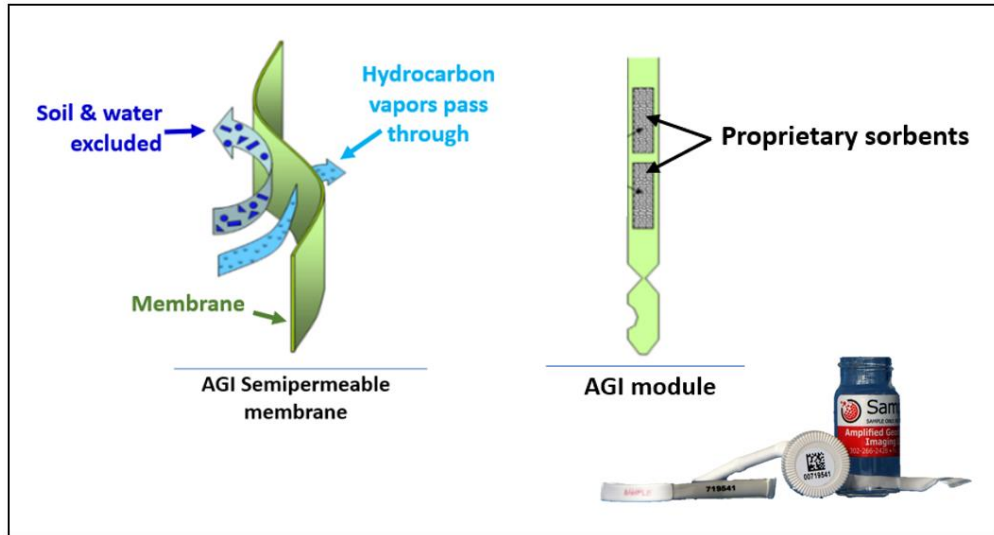


Figure 4. The proprietary ultrasensitive passive geochemical module excludes extraneous materials and allows organic compounds to pass through the membrane and concentrate on the specially engineered sorbents within. These sorbents not only trap the hydrocarbon compounds from  $C_2 - C_{20}$ , but also concentrate them resulting in a detection 1,000-times lower than conventional geochemical methods.

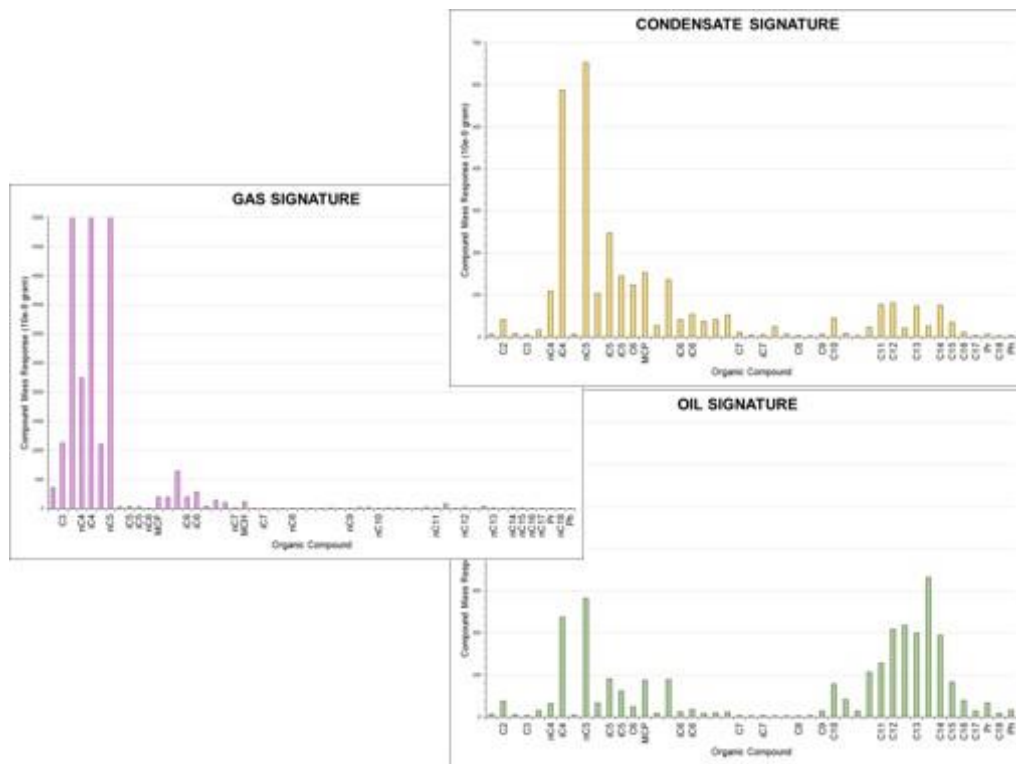


Figure 5. The ability of the ultrasensitive geochemical method to capture compounds from the  $C_2 - C_{20}$  range provides the unique ability to clearly differentiate hydrocarbon signatures as gas, gas condensate, or oil. Traditional geochemical methods do not measure the gas condensate range from  $C_6 - C_{15}$ .

## Methodology Trials

The initial trials for the concept began by placing ultrasensitive modules in saline water in pressure vessels at 150 bar & 300 bar (i.e. equivalent to ~1500 m & ~3000 m depth) to:

1. evaluate potential distortion effects of the passive adsorbents within the module;
2. determine if pressure affected hydrocarbon assimilation over the  $C_2 - C_{20}$  range;
3. evaluate the effect of saline water intrusion into the modules.

As seen in Figure 6, the spiked sample Total Ion Chromatogram (TIC) signature documents the ability of the sorbers to function properly under extreme pressure and adsorb hydrocarbons. The hydrocarbon range, from  $C_2 - C_{20}$ , and the hydrocarbon pattern in the tested samples were similar to the analytical standards analyzed during the analytical instrument sequence. The blank signature also indicated that there was no degradation of the sorbent material during the trials. It was also determined that saline water intrusion effects could be minimized prior to analysis.

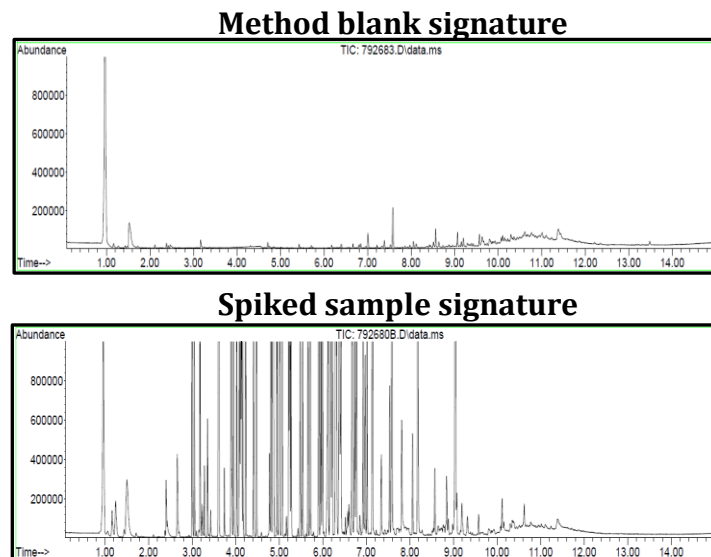


Figure 6. The hydrocarbon signatures illustrate that the geochemical passive sorbers were functioning properly within the high-pressure vessels in brine solutions. The upper signature shows the analytical signature of passive module in the high-pressure vessel where no hydrocarbons have been added. The second fingerprint indicates the result of the test where 100 ng of hydrocarbons have been added to the pressure vessel. The result indicates good adsorption of the hydrocarbons by the passive module even under 300 bar of pressure.

Field trials were performed in offshore Ghana, see Figure 7. The module testing coincided with evaluation of a new OBS node. As such, the trial was not intended to duplicate normal field operations, but rather provide an assessment of whether the geochemical modules could function properly under field conditions.

The passive modules were attached to the bottom of the OBS nodes. When lowered to the seabed floor, the weight of the Ocean Bottom Nodes (OBN) pressed the geochemical module into the seafloor sediment. The samples were deployed for less than a week. Normal deployment would be for between 3 – 6 weeks.

Survey fingerprints are shown in Figure 8. Nodes 2000 & 1348 show examples of positive thermogenic signatures. The positive signatures contrast sharply to the baseline signature for Node 1461. The baseline signature for Node 1461 demonstrates that the positive signatures were thermogenic in nature and not from



shipboard contamination. Thus, the field trial validated that the ultrasensitive sorbers could be deployed on OBS nodes to detect ultralow levels of reservoir hydrocarbons. Note that a normal deployment duration of 3 – 6 weeks is expected to increase hydrocarbon intensity on the passive geochemical modules.

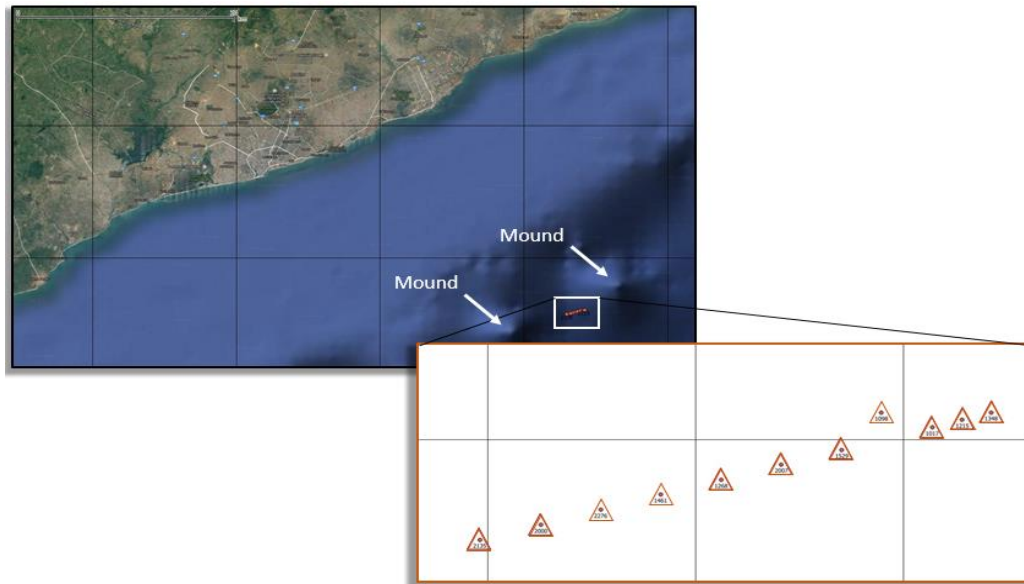


Figure 7. This figure illustrates the sampling location for the module testing in offshore Ghana. Eleven modules were tested by placing them on the bottom of heavy OBS nodes. The nodes were lowered onto the seabed floor which pressed the modules into the seafloor sediment. Note, the mud mounds near the sampling location that is typically indicate of petroleum systems.

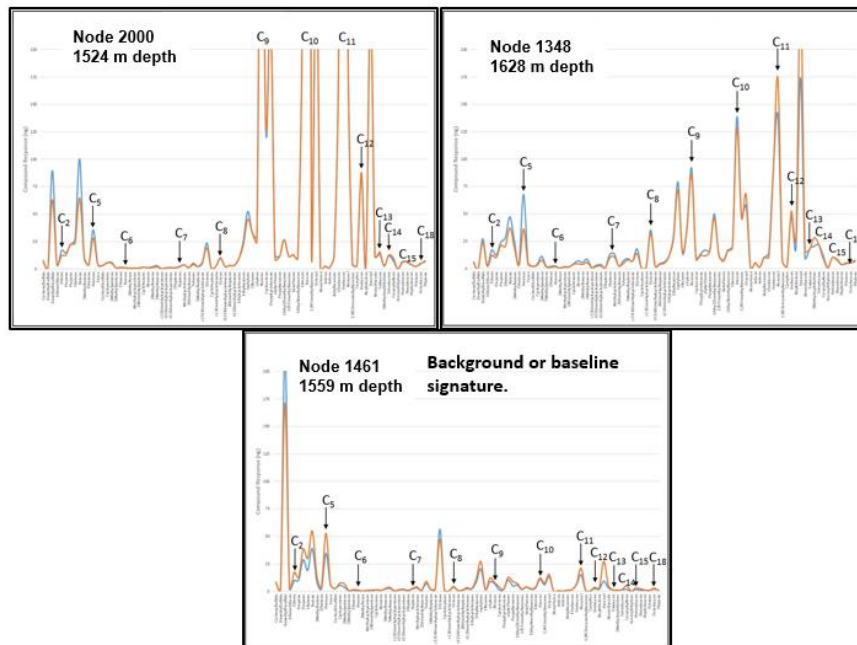


Figure 8. Nodes 2000 & 1348 show examples of positive thermogenic signatures. The positive signatures contrast sharply to the baseline signature for Node 1461. The baseline signature for Node 1461 demonstrates that the positive signatures were thermogenic in nature and not from shipboard contamination.

## Case Study Example

This earlier case study (Schrynmeeckers, 2013; Schrynmeeckers, 2016) is intended to illustrate how the geochemical data from the joint geochemical/OBS node capability can be utilized for offshore field development purposes. The surface surveys took place in the Anadarko Basin in Oklahoma, USA. The purpose of the survey was to map over-pressured gas condensate from the Pennsylvanian Red Fork channel sands from a depth of ~14,000 ft. The data set encompassed nine surveys over 120 mi<sup>2</sup> for a three-year period. One of the difficulties of the project was that the Anadarko Basin includes numerous oil and gas charged horizons throughout the Paleozoic section.

The resulting geochemical survey probability map is seen in Figure 9. The probability factor is the probability of finding Red Forks channel sands gas condensate. The red shading indicates areas with a high probability factor (i.e. ~85% - 95% probability), while the yellow represents low probability. The purple line outlines the boundaries of the survey areas.

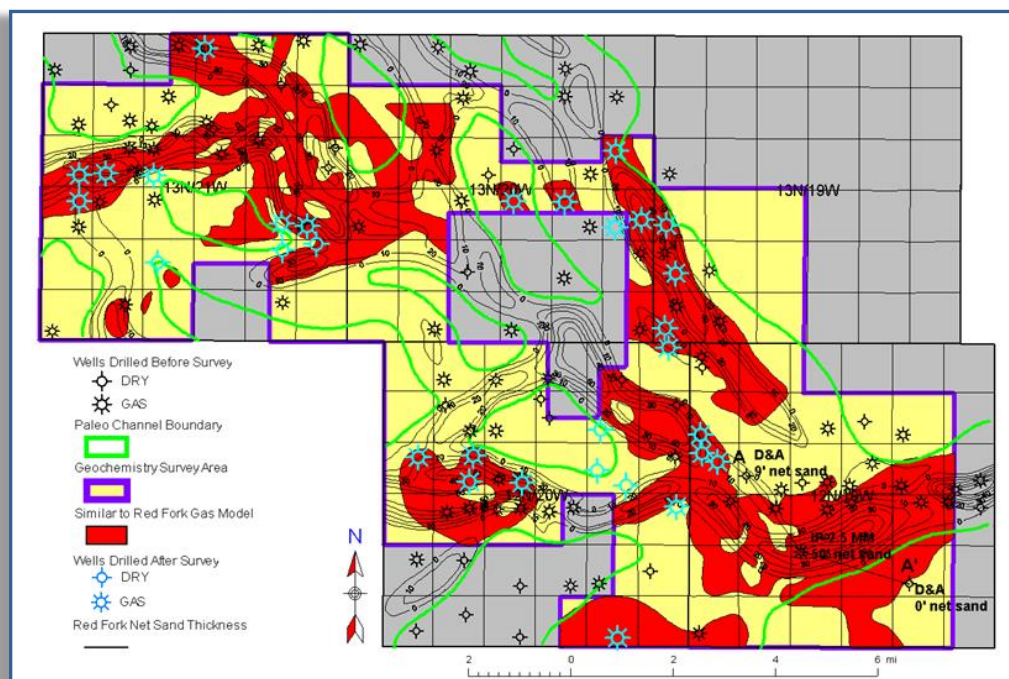


Figure 9. The map shows the results from the geochemical survey. The red indicates areas with an 85% - 95% probability of finding hydrocarbons similar to the Red Fork channel sand gas condensate. The yellow represents poor probability. Gray shaded areas were not included in the survey. The light blue production well symbols indicate wells drilled post-survey. The black production well symbols indicate wells drilled prior to the surveys. Note many of these wells are in yellow, nonprospective or noneconomic, areas. This is due to the fact these wells are in the latter stages of their production life and have depleted pressure and depleted hydrocarbon volumes.

The light blue producing well symbols indicate wells drilled post-survey. Note, the majority of these wells are found on the red shaded areas indicating a high probability of gas condensate presence. Several older producing wells are found in yellow and gray, non-prospective, areas. The time-lapse geochemistry is reflecting reduced hydrocarbon volume and reduced pressure (i.e. depletion effects) for these wells, and thus correctly identifies them as noneconomic. As multiple geochemical surveys are performed with modules placed in reoccurring locations, the geochemical probability maps can also illuminate the movement of hydrocarbons over time (i.e. time lapse geochemistry).

Figure 10 shows a graph plotting the geochemical probability factor on the Y axis versus porosity times net



pay ( $\phi$ -h) on the X axis. The plot shows a strong correlation (i.e.  $r^2 = 0.87$ ) between effective porosity ( $\Phi$ ), net pay thickness (h), and the surface geochemical expression. The graph shows dry wells and sub-economic wells with poor probability factors ranging from ~50% - 60% and poor  $\phi$ -h, while the wells with higher probability factors exhibit improved  $\phi$ -h. Thus, the graph demonstrates the ability of the ultrasensitive hydrocarbon data to map areas of higher porosity and net pay thickness (i.e. Sweet Spots).

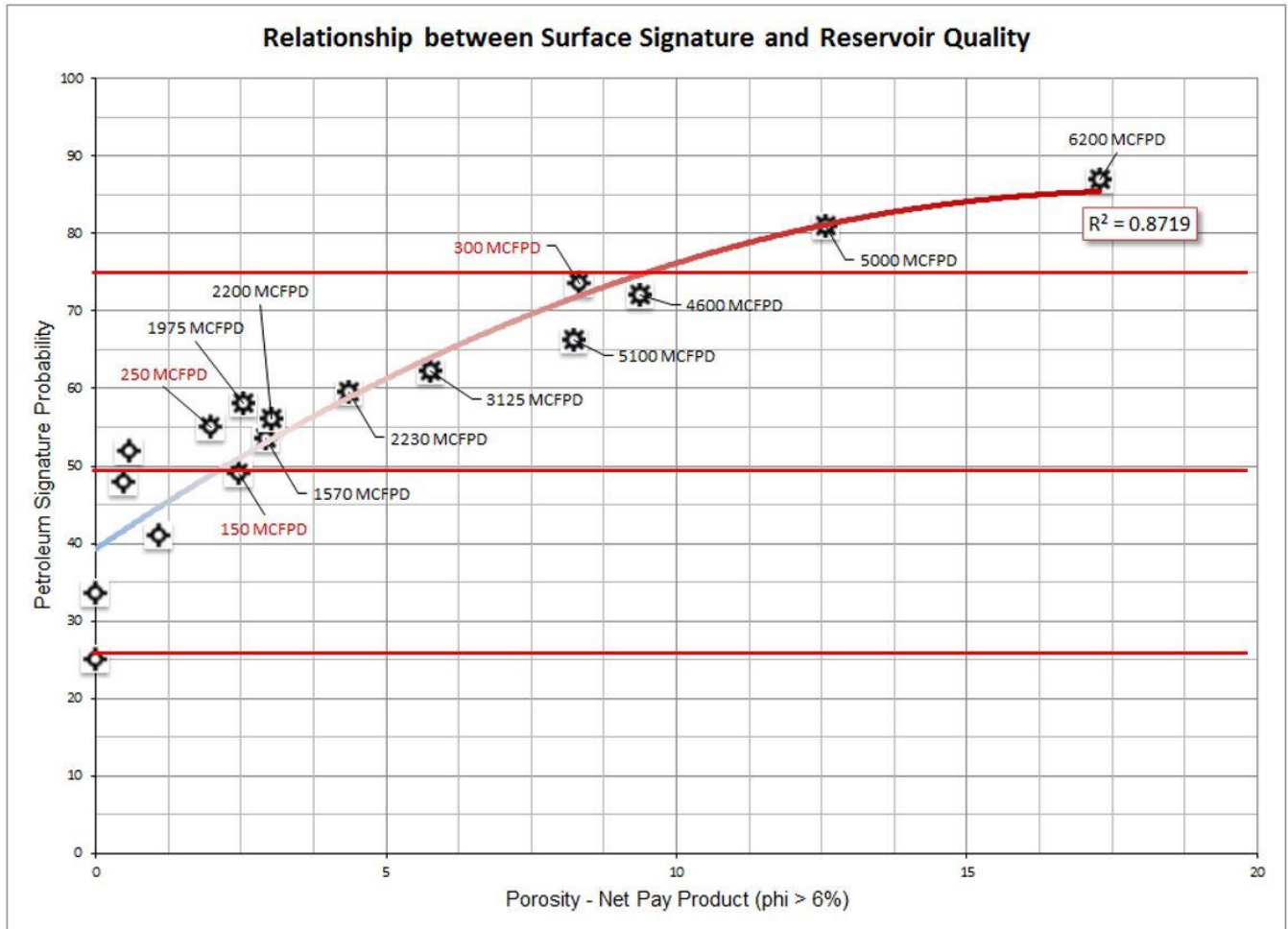


Figure 10. The graph plots the geochemical probability factor vs  $\phi$ -h. The higher the probability factor the better the chance of incurring productive Red Fork channel sands. Note the strong correlation (i.e.  $r^2 = 0.87$ ) between effective porosity ( $\Phi$ ), net pay thickness (h), and the surface geochemical expression. This results from the fact that pressure, porosity, and net pay thickness drive microseepage. Also note, the greater the geochemical probability factor the greater the production.

Note also the strong correlation with the geochemical probability factors and production. Field production increases proportionally with the geochemical probability values. Geochemical probability factors between 50% - 60% correlated with an average production of 1,396 MCFPD. Geochemical probability factors between 60% - 70% correlated with an average production of 4,275 MCFPD. The 81% probability factor showed 5,000 MCFPD production and the 87% probability factor reflected 6,200 MCFPD production.

The graph can also identify potential suboptimal completions. For example, the well reporting only 300 MCFPD had an elevated probability factor (i.e. ~73%) and a healthy  $\phi$ -h, suggesting possible untapped behind-the-pipe pay.

Geochemical results were ground-truthed by post-survey drilling. Thirty (30) post-survey wells were drilled:

- 22 wells were drilled on positive geochemical anomalies for Red Fork gas condensate, with 21 commercial discoveries and 1 dry well;
- 8 wells were drilled out of anomalies (no hydrocarbons) of which 5 plugged and abandoned and one failed to pay completion cost. Two were gas condensate discoveries.

Consequently, the ultrasensitive geochemical survey correctly predicted 90% (27 of 30) of the post-survey well results.

## Conclusions

This combination of exploration technologies can provide unique capabilities that have not been available in the industry previously. This is the first time that high resolution seismic imaging and petroleum system hydrocarbon data can be acquired at the same locations simultaneously, which is critical for field development applications particularly where routine monitoring is performed. This tandem capability allows for optimizing reservoir understanding that reflects subsurface reality.

For example, the combined data sets will be able to:

- identify compartmentalization;
- map hydrocarbon movement over time;
- map depletion effects;
- map reservoir sweet spots (i.e. areas of higher porosity, pressure, & hydrocarbon richness);
- rank prospects;
- reduce risk by identifying poor prospectivity areas;
- accurately map hydrocarbon charge through thick salt sequences (Schrynemeekers and Gharib, 2016);
- augment seismic data in highly thrust and faulted areas.

## References

- Araktingi, R. E., Benefield, M. E., Bessenyei, z., Coats, K. H., and Tek, M. R., 1984, Leroy storage facility, Uinta County, Wyoming: a case history of attempted gas-migration control. *Journal of Petroleum Technology*, v. 34, 132 – 140.
- Davidson, M. J., 1982, Toward a general theory of vertical migration. *Oil and Gas Journal*, v. 80, no. 25, 288 – 300.
- Davidson, M. J., 1985, Overview on vertical migration and surface expression of petroleum, *in* Surface and near-surface geochemical methods in petroleum exploration, R. W. Klusman, coordinator, Association of Petroleum Geochemical Explorationists, Special Publication No. 1, Denver CO, B1 – 16.
- Jones, V. T., and Burtell, S. G., 1996, Hydrocarbon flux variations in natural and anthropogenic seeps, *in* D. Schumacher and M. Abrams, eds., Hydrocarbon migration and its near-surface expression: AAPG Memoir 66, 203 – 221.
- Klusman, R., 1993, Soil gas and related methods for natural resource exploration: New York, New York, John Wiley and Sons Publishers, 483.
- Klusman, R., and Saeed, M., 1996, Comparison of light hydrocarbon microseepage mechanisms, *in* D. Schumacher and M. Abrams, eds., Hydrocarbon migration and its near-surface expression: AAPG Memoir 66, 157 – 168.
- Price, L. C., 1986, A critical overview and proposed working model of surface geochemical exploration, *in* M. J. Davidson, ed., Unconventional methods in exploration for petroleum and natural gas, IV: Dallas, Texas, Southern Methodist University Press, 245 – 309.
- Rice, G. K., 1986, Combined near-surface geochemical and seismic methods for petroleum exploration, evidence for vertical migration. *Association Petroleum Geochemical Explorationists Bulletin*, v. 2, 46 – 62.
- Rostron, B. J., and Toth, J., 1996, Ascending fluid plumes above Devonian pinnacle reefs: numerical modeling and field example from west-central Alberta, Canada, *in* D. Schumacher and M. Abrams, eds., Hydrocarbon migration and its near-surface expression: AAPG Memoir 66, 185 – 201.

- 
- Saunders, D. F., Burson, K. R., and Thompson, C. K., 1999, Model for hydrocarbon microseepage and related near-surface alterations: AAPG Bulletin, v. 83, 170 – 184.
- Schrynmeeckers, R., 2011, Minimizing Offshore Exploration Risks by Evaluating the Charge of Subsea Structures, Subsea Survey Conference, Galveston, TX.
- Schrynmeeckers, R., 2013, Using Surface Hydrocarbon Mapping to Derisk Field Development Efforts, AAPG Geoscience Technology Workshop – Revisiting Reservoir Quality Issues in Unconventional and Conventional Resources, Austin, TX.
- Schrynmeeckers, R., 2016, Increasing Production in Mature Fields While Reducing Costs, AAPG Geoscience Technology Workshop – Making Money in Mature Fields, Houston, TX.
- Schrynmeeckers, R., and Gharib, J., 2016 Improving Petroleum System Identification in Offshore Salt Environments: Gulf of Mexico and Red Sea case Studies, Offshore Technology Conference, Houston, TX, OTC-26897-MS.
- Silliman, A.H., 2005, Hydrocarbon Compound Microseepage and Vertical Migration with Evidence from the GORE Survey for Exploration, Internal Whitepaper, W.L. GORE & Associates.